nature immunology

Dock8 mutations cripple B cell immunological synapses, germinal centers and long-lived antibody production

Katrina L Randall[1,2,10], Teresa Lambe[3,10], Andy Johnson[3,4], Bebhinn Treanor[5], Edyta Kucharska[1], Heather Domaschenz[1], Belinda Whittle[1], Lina E Tze[1], Anselm Enders[1], Tanya L Crockford[3], Tiphaine Bouriez-Jones[3], Duncan Alston[3], Jason G Cyster[6], Michael J Lenardo[7], Fabienne Mackay[8], Elissa K Deenick[9], Stuart G Tangye[9], Tyani D Chan[9], Tahra Camidge[9], Robert Brink[9], Carola G Vinuesa[1], Facundo D Batista[5], Richard J Cornall[3,10] & Christopher C Goodnow[1,10]

To identify genes and mechanisms involved in humoral immunity, we did a mouse genetic screen for mutations that do not affect the first wave of antibody to immunization but disrupt response maturation and persistence. The first two mutants identified had loss-of-function mutations in the gene encoding a previously obscure member of a family of Rho-Rac GTP-exchange factors, DOCK8. DOCK8-mutant B cells were unable to form marginal zone B cells or to persist in germinal centers and undergo affinity maturation. *Dock8* mutations disrupted accumulation of the integrin ligand ICAM-1 in the B cell immunological synapse but did not alter other aspects of B cell antigen receptor signaling. Humoral immunodeficiency due to *Dock8* mutation provides evidence that organization of the immunological synapse is critical for signaling the survival of B cell subsets required for long-lasting immunity.

Antigen receptor signaling coordinates the antibody response to infection or immunization, but the nature of the signals that guide the formation of high-affinity memory B cells and long-lived humoral immunity remains unclear. Two classes of antibody-deficiency syndromes are now recognized as arising from defects in antigen receptor signaling: defects in early B cell development and common variable immunodeficiency (CVID)[1]. Defects in early B cell development result from mutations in genes encoding the components of the B cell antigen receptor (BCR) and the Bruton's tyrosine kinase signaling cascade immediately downstream. These syndromes are readily identified by agammaglobulinemia and lower numbers of circulating B cells. In contrast, CVID syndromes have relatively normal B cell numbers and may have qualitative or quantitative defects in immunoglobulin production[2]. CVID is the most common clinically important primary immunodeficiency, yet over 75% of cases cannot be explained genetically or mechanistically at present[3]. A small number of cases result from mutations in the gene encoding CD19 (A000538)[4], a coreceptor for enhancing BCR signaling that recruits phosphatidylinositol-3-OH kinase (PI(3)K; A001770)[5]. Other subsets are due to mutations in the gene encoding TACI, which is one of the receptors for the tumor necrosis factor–related cytokines BAFF and APRIL[6,7], or mutations in the gene encoding ICOS, which serves as a costimulatory receptor for follicular helper T cells[8]. Understanding the variable antibody responses and deficiencies of switched memory B cells in the CVID spectrum of disorders[9] is hindered by the limited understanding of the genes and signaling mechanisms that are specifically required for the maturation and longevity of the antibody response.

To identify additional genes and mechanisms that generate mature antibody responses, and animal models for understanding CVID and related immunodeficiencies, we describe here an immunization screen for selective defects in antibody-response maturation and longevity in mouse pedigrees segregating thousands of induced single-nucleotide substitutions. The first two pedigrees with humoral immune deficiency identified by this screen resulted from independent mutations in *Dock8*, which encodes a previously obscure member of the DOCK family of Rho-Rac guanine-exchange factors. The consequences of this mutation in B cells provide evidence that polarization of lymphocyte antigen receptors and integrins into an immunological synapse is critical for signaling survival and

[1]John Curtin School of Medical Research and Australian Phenomics Facility, Australian National University, Australia. [2]Department of Immunology, The Canberra Hospital, Garran, Australian Capital Territory, Australia. [3]Nuffield Department of Clinical Medicine, Oxford University, Oxford, UK. [4]Laboratory of Cellular and Molecular Immunology, and [7]Laboratory of Immunology, National Institute of Allergy and Infectious Disease, National Institutes of Health, Bethesda, Maryland, USA. [5]Cancer Research UK, London Research Institute, Lincoln's Inn Fields, London, UK. [6]Howard Hughes Medical Institute and Department of Microbiology and Immunology, University of California, San Francisco, California, USA. [8]Department of Immunology, Faculty of Medicine, Nursing and Health Sciences, Monash University, Melbourne, Victoria, Australia. [9]Garvan Institute of Medical Research, Darlinghurst, New South Wales, Australia. [10]These authors contributed equally to this work. Correspondence should be addressed to C.C.G. (chris.goodnow@anu.edu.au) or R.J.C. (richard.cornall@ndm.ox.ac.uk).

Received 15 September; accepted 1 October; published online 8 November 2009; doi:10.1038/ni.1820

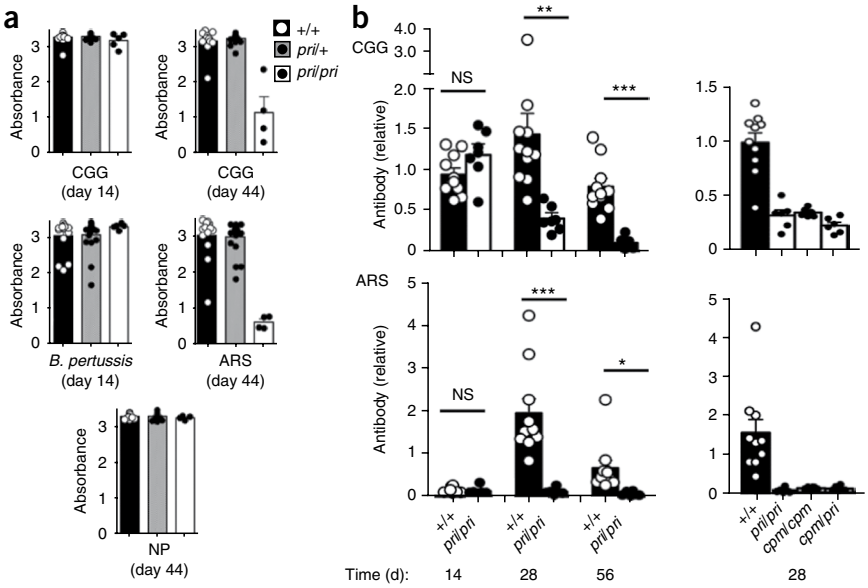

Figure 1 Identification of two independent, noncomplementing *N*-ethyl-*N*-nitrosourea–mutant mouse strains with humoral immunodeficiency characterized by failure to sustain a primary immune response and failure of maturation of the antibody response. (**a**) Screening assay: enzyme-linked immunosorbent assay of IgG1 antibody to CGG and ARS, IgM antibody to nitrophenyl (NP), and IgG2c antibody to *B. pertussis* in serum collected from wild-type (+/+), *pri*/+ and *pri*/*pri* mice 14 d after primary immunization (day 14) and 6 d after booster immunization (day 44), presented as absorbance. For the detection of low responders among large numbers of mice, serum was tested at a fixed dilution, which yielded sub-saturating antibody titers in wild-type mice (CGG, 1/2,000 and 1/20,000; BP, 1/50; nitrophenyl, 1/50; ARS, 1/2,000). Each symbol represents an individual mouse. (**b**) Longitudinal monitoring of antibody titers to CGG and ARS at 14, 28 and 56 d after primary immunization, determined by titration of each serum sample against the titer of a standard reference serum, set as 1. Each symbol represents an individual mouse. NS, not significant; $*P < 0.05$; $**P < 0.005$; $***P < 0.0005$ (Student's *t*-test). Data are representative of three independent experiments (arithmetic mean and s.e.m.).

the establishment of high-affinity antibody-producing cells and long-lasting immunity, and yield a timely animal model for understanding human immunodeficiency.

RESULTS

Immunization screen

To understand the generation of long-lived humoral immunity, we developed a genetic screen that could identify mutant mice with a failure to mount long-lived, high-affinity antibody responses despite a relatively normal initial wave of antibody production. We tested 301 pedigrees of C57BL/6 mice, each segregating thousands of *N*-ethyl-*N*-nitrosourea–induced single-nucleotide substitutions, for initial and mature serum antibody after immunizing multiple siblings of each pedigree with a mixture of antigens. Two recessive mutations that disrupted antibody response maturation (**Fig. 1**) were propagated from independent pedigrees (called '*captain morgan*' (*cpm*) and '*primurus*' (*pri*) here). During the initial antibody response, immunoglobulin G (IgG) antibodies to killed *Bordetella pertussis* bacteria and to the protein antigen chicken γ-globulin (CGG) were correctly polarized to IgG2c and IgG1, respectively, and reached indistinguishable titers 14 d after immunization of *pri*/*pri* homozygous mice, *cpm*/*cpm* mice and their wild-type siblings (**Fig. 1a**, top, **1b** and data not shown). As the majority of antibodies to CGG and *B. pertussis* produced at this time come from extrafollicular B cell clonal expansion and plasma cell formation acting together with T helper type 1 (T_H1) and T_H2 T cells in the T cell zone[10], the absence of a substantial effect of the mutations on this phase of antibody production established that this phase of B cell and T cell activation was intact. The homozygous mutations also did not have an appreciable effect on T cell–independent (TI-2) extrafollicular B cell responses to nitrophenyl-hapten coupled to the polysaccharide antigen Ficoll (**Fig. 1a**). However, during the mature phase of the antibody response, either after a booster immunization (44 d; **Fig. 1a**) or without boosting (28 or 56 d after primary immunization; **Fig. 1b**), IgG antibody to CGG failed to be sustained in *pri*/*pri* or *cpm*/*cpm* mice or in compound-heterozygous mice. The CGG immunogen carried a haptenic chemical group, azobenzenearsonate (ARS), which elicited appreciable antibody only in wild-type mice after 4 weeks (**Fig. 1b**) due to the need for antibody hypermutation and affinity maturation[11,12]. Antibody to the ARS hapten failed to develop in *pri*- or *cpm*-homozygous mice or compound-heterozygous mice.

A comprehensive analysis of B cell subsets in blood and primary and secondary lymphoid organs showed qualitatively normal development of circulating mature subsets but a near absence of marginal zone B (MZB) cells (**Fig. 2**). The formation of immature B cells in the bone marrow and accumulation of mature follicular B cells seemed normal in mutant mice (**Fig. 2a**,**b** and data not shown), but there was profound deficiency of splenic MZB cells in *cpm*- and *pri*-homozygous mice and *cpm*/*pri* compound-heterozygous mice (**Fig. 2a–d** and **Supplementary Fig. 1**), which was cell autonomous to B cells bearing the mutation in mixed chimeras (**Fig. 2e**). MZB cell numbers were much higher in transgenic mice overexpressing the cytokine BAFF, but this failed to restore MZB cell formation by mutant cells (**Supplementary Fig. 2**). The frequency of B-1 cells in the peritoneal cavity was 60% lower in the mutant mice (**Fig. 2f**), and this was cell autonomous in mixed chimeras. Analysis of splenic T cells showed normal numbers of activated or memory $CD4^+$ and $CD8^+$ T cells but a mean 50% lower number of naive T cells in *cpm*- and *pri*-homozygous mice and in *cpm*/*pri* compound-heterozygous mice, although this trait overlapped the lower end of the normal range and was not reliable for identifying individual homozygous mice (**Fig. 2g**). In 50:50 bone marrow chimeras with mutant T cells reconstituting in the presence of wild-type T cells, T cells bearing the mutation had a cell-autonomous competitive disadvantage and comprised only 5% of the total peripheral T cells (**Fig. 2h**).

Dock8 mutations

MZB cell deficiency provided a clear mendelian recessive trait to map and identify the causative *cpm* and *pri* mutations. Both mutations mapped to the same region of chromosome 19 (**Supplementary Fig. 3**), and sequencing of B cell–expressed transcripts in the minimal 4.5-megabase interval identified independent mutations in *Dock8*

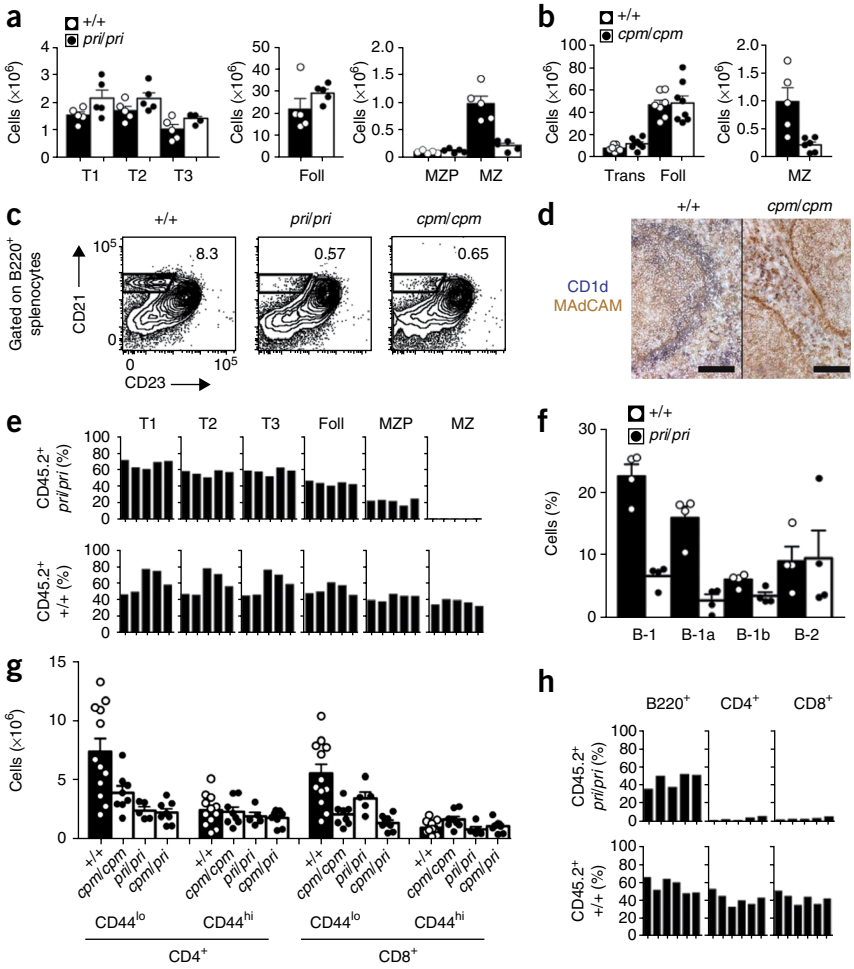

Figure 2 Analysis of splenic and peritoneal lymphocyte subsets. (**a**,**b**) Immature transitional B cells (T1–T3 or Trans), mature follicular B cells (Foll), MZB cell precursors (MZP) and MZB cells (MZ) in spleens of wild-type mice (**a**,**b**), *pri*/*pri* mice (**a**) and *cpm*/*cpm* mice (**b**). $P = 0.006$ (**a**) and $P = 0.038$ (**b**), MZB cell numbers; other B cell subset differences not statistically significant (unpaired two-tailed *t*-test). (**c**) Flow cytometry of B cells in the MZB cell subset. Numbers adjacent to outlined areas indicate percent B cells. (**d**) Immunohistochemistry of the splenic MZB cell marker CD1d and marginal sinus marker MAdCAM in spleen sections from wild-type and *cpm*/*cpm* mice. Scale bar, 50 μm. (**e**) Reconstitution of B cell subsets (above plots) in the spleens of mixed-chimera mice by mutant (*pri*/*pri*) or wild-type CD45.2$^+$ cells. Representative of two separate cohorts of *pri*/*pri* mixed chimeras and two cohorts of *cpm*/*cpm* mixed chimeras. (**f**) Frequency of B-1, B-1a, B-1b and B-2 subsets in the peritoneum of wild-type and *pri*/*pri* mice. (**g**) Number of splenic T cells in wild-type, *cpm*/*cpm*, *pri*/*pri* and *cpm*/*pri* mice. $P = 0.0003$, naive (CD44^{lo}) CD4$^+$ T cells, and $P = 0.0001$, naive (CD44^{lo}) CD8$^+$ T cells (analysis of variance); $P = 0.048$, CD8CD44^{hi} cells (CD4CD44^{hi} cells, not significant). (**h**) Reconstitution of splenic cell subsets of mixed chimeras by mutant or wild-type CD45.2$^+$ cells. Each symbol represents an individual mouse (**a**,**b**,**f**,**g**). Each bar in **e**,**h** represents an individual mouse. Data are representative of two (**a**,**b**,**d**,**f**), three (**e**,**g**,**h**) or more than five (**c**) independent experiments (mean and s.e.m. in **a**,**b**,**f**,**g**).

(**Fig. 3a**). DOCK8 is a little studied member of a family of proteins that are critical activators of the Rho family of small GTPases (G proteins) in worms, flies and mammals[13]. In other DOCK proteins, the DOCK-homology region 1 (DHR1) domain (also known as the CDM-zizimin homology 1 (CZH1) domain) binds phosphatidylinositol-3,4,5-triphosphate (PtdIns(3,4,5)P_3) lipids generated by PI(3)K activity to promote localized membrane binding and activation. The DHR2 (CZH2) domain binds to Rho-family G proteins (Rho (A002062), Rac and Cdc42), promoting GTP exchange and activating local cytoskeletal changes, integrin-mediated adhesion, lamellipodia formation, cell polarization, phagocytosis or cell fusion[13,14]. DOCK8 has been isolated in a yeast two-hybrid screen for binding partners of Cdc42 and has been found to localize at lamellipodia in fibroblasts[15], but its *in vivo* function has remained unknown.

The *cpm* mutation was a T-to-C substitution in the exon-20 splice-donor sequence that caused aberrant mRNA splicing between cryptic 5′ or 3′ splice donors and the normal exon 21 splice acceptor (**Fig. 3b**,**c**). Sequencing of 74 cDNA clones from *cpm*/*cpm* splenocytes showed aberrant splicing to yield frameshifts and premature stop codons that eliminate the DHR2 domain entirely (**Fig. 3c**). The *pri* mutation, in exon 43, was a T-to-C substitution that changed codon 1827 from a serine residue to a proline residue (**Fig. 3a**). The mutant serine residue was absolutely conserved in vertebrate DOCK8 and in the DHR2 domain of DOCK6, DOCK7 and DOCK9 (**Fig. 3d**). In the structure of DOCK9 in complex with Cdc42 (ref. 16), this conserved serine lies in DHR2 lobe B α-helix 6, which forms part of the Cdc42-binding site and provides four Cdc42 contact residues (**Fig. 3d**). The *pri* substitution of Ser1827 to Pro1827 would be expected to break this α-helical structure and interfere with the guanine-exchange factor activity of the DHR2 domain. The nature of the mutations, their recessive inheritance and their failure to complement in crosses established the cause of the antibody response, B cell and T cell defects as being due to loss of normal DOCK8 function. *Dock8* mRNA was expressed ten times more abundantly in B lymphocytes and T lymphocytes than in other cells (**Supplementary Fig. 4**). As mice homozygous for the truncating *Dock8*^{cpm} allele are weaned at normal frequency and seem normal in growth and behavior, we conclude that DOCK8 has a relatively specialized role in adaptive immunity.

Crippled germinal centers

As immunization of DOCK8-mutant mice elicited a normal early wave of antibody formation but the response failed to mature or be sustained, we sought to define the cellular basis for this variable immune deficiency. After immunization with sheep red blood cells (SRBCs), wild-type mice formed large germinal centers (GCs), indicated by peanut agglutinin–positive (PNA$^+$) IgD$^-$ B cells, whereas *pri*/*pri* and *cpm*/*cpm* mice formed only small PNA$^+$ clusters (**Fig. 4a** and data not shown). Phenotypically normal CD95$^+$GL7$^+$B220$^+$ GC B cells were readily detected by flow cytometry in homozygous mutants after immunization, but their numbers were only 15% of normal (**Fig. 4b**). Immunization of competitive hematopoietic chimeras,

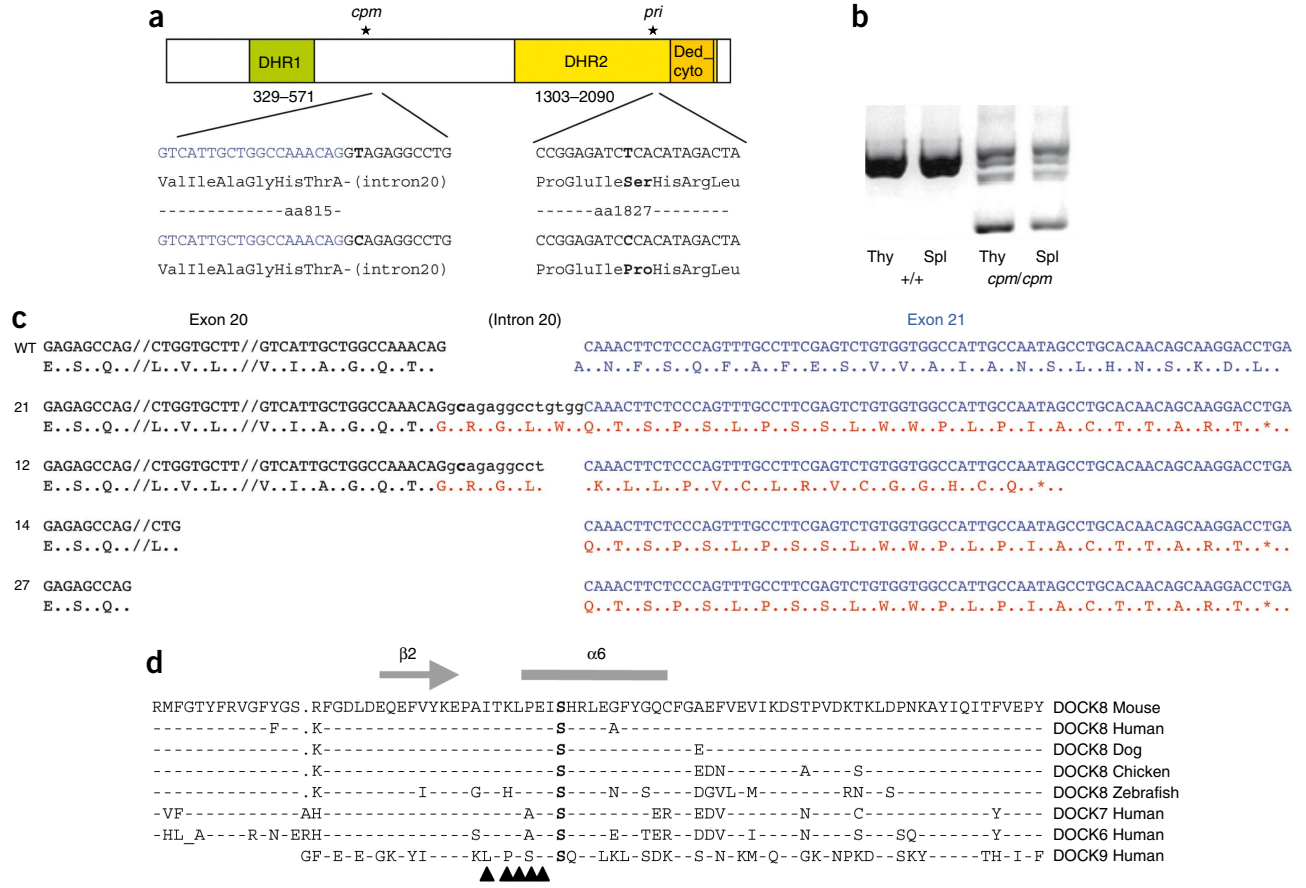

Figure 3 Independent *Dock8* mutations in *pri* and *cpm* mouse strains. (**a**) Conserved *Dock8* domains; stars and bolding indicate position of mutations. Ded-cyto, subdomain pfam0692 of DHR2. (**b**) Amplification products of cDNA of *Dock8* exons 18–21 from thymus (Thy) and spleen (Spl) of wild-type and *cpm*/*cpm* mice. Data are representative of four independent experiments. (**c**) Sequence of cDNA clones from the *cpm*/*cpm* mice in **b**, aligned with the wild-type *Dock8* cDNA sequence. Left margin, number of clones of each type. '//' indicates omission of segment of normal exon 20 sequence. (**d**) Sequence alignment of DOCK8 orthologs and paralogs in the region surrounding sequence encoded by the *pri* mutation. Mutant serine is in bold; dashes indicate identity to mouse DOCK8; grey arrow and underlining (above) indicate position of β2 and α6 secondary structure elements, based on DOCK9 structure[16]; upward arrowheads (below) indicate Cdc42-contact residues in DOCK9 (ref.16).

constructed by reconstitution of irradiated mice with a mixture of CD45.1$^+$ wild-type and CD45.2$^+$ *pri*/*pri* or *cpm*/*cpm* bone marrow, showed that B cells bearing the *Dock8* mutation contributed normally to the main subsets of B220$^+$ and IgD$^+$ recirculating follicular B cells but contributed poorly to the B220$^+$CD95$^+$GL7$^+$ GC subset, particularly at day 11 after immunization, when the response has begun maturing (**Fig. 4c**). The mutations therefore acted autonomously in individual B cells to interfere selectively with their capacity to differentiate into or sustain a GC state.

We determined the precise step at which the mutation interfered with GC B cells by monitoring a homogeneous population of B cells specific for hen egg lysozyme (HEL) antigen after adoptive transfer into wild-type mice immunized with SRBCs conjugated to HEL (**Figs. 5** and **6**). We crossed mice with the *pri* mutation with CD45.1 SW_{HEL}-transgenic mice, which bear a rearranged HEL-specific variable-diversity-joining heavy-chain ($V(D)J_H$) element targeted to the *Igh* locus (which encodes the immunoglobulin heavy chain) combined with a HEL-specific κ-light-chain transgene[17]. We adoptively transferred B cells from *pri*/*pri* CD45.1$^+$ SW_{HEL}-transgenic donors, or from wild-type CD45.1$^+$ SW_{HEL}-transgenic controls, into wild-type C57BL6 (CD45.2$^+$) recipients. We then immunized the recipients with a conjugate antigen composed of SRBCs covalently 'decorated' with HEL protein bearing two substitutions (HEL^{2X}). In contrast to the very high affinity of immunoglobulin receptors on SW_{HEL} B cells for native HEL (2×10^{10} M^{-1}), HEL^{2X} is recognized with intermediate affinity (8×10^7 M^{-1}) by immunoglobulin receptors on SW_{HEL} B cells due largely to the effect of the Asp101-to-Arg101 substitution[18–20]. Six amino acids in the complementarity-determining region 2 (CDR2) loop of the SW_{HEL} V_H chain contact native HEL at Asp101 (ref. 21), and selection of amino acid replacements in these CDR2 residues increases the affinity for D101R-substituted HEL^{2X} or HEL^{3X} antigens in SW_{HEL} GC cells (ref. 19 and unpublished data).

In wild-type recipients immunized with HEL^{2X} SRBCs, both wild-type and *pri*/*pri* HEL-specific B cells underwent similar differentiation into GL7$^+$Fas$^+$ cells scattered in follicles 2.5 d after immunization, and similar rates of isotype switching to IgG1 occurred between days 3.5 and 4.5 (**Fig. 5** and **Supplementary Fig. 5**). GCs formed in follicles on day 4.5, when the majority of both wild-type and mutant SW_{HEL} B cells had differentiated into Fas^{hi}GL7^{hi} GC cells. No accumulation or GC differentiation by donor B cells occurred in recipients immunized with SRBCs lacking the HEL^{2X} antigen. Immunoglobulin class switching is a sensitive indicator of helper T cell signals[22] and requires CD40 on SW_{HEL} B cells in immune responses to HEL^{2X} SRBCs[23]. These data reinforce those presented above (**Fig. 1**) in indicating that DOCK8 is not essential for the initial phase of B cell activation and functioning together with helper T cells *in vivo*.

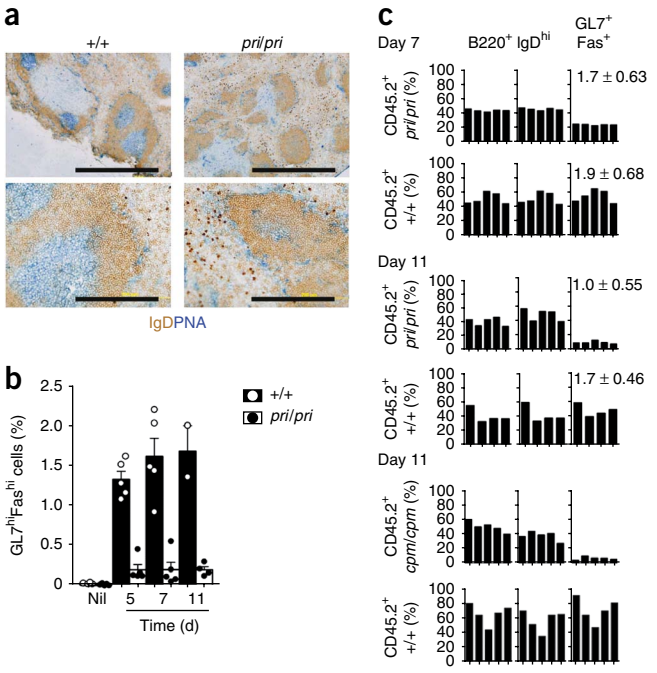

Figure 4 *Dock8* mutation causes an intrinsic defect in GC B cells. (**a**) Immunohistochemistry of splenic PNA$^+$ GCs and IgD$^+$ follicular mantle 7 d after immunization with SRBCs. Scale bars, 500 μm (top row) or 200 μm (bottom row). (**b**) Frequency of GC B cells in untreated mice (Nil) or in mice at 5, 7 and 11 d after immunization with SRBCs, presented as a percentage of B220$^+$ cells. Each symbol represents an individual mouse. Data are representative of four independent experiments (one per time point; arithmetic mean and s.e.m.). (**c**) Contribution of CD45.2$^+$ cells from wild-type, *pri/pri* and *cpm/cpm* mice to B cell subsets in 50:50 mixed–bone marrow chimeras 7 or 11 d after immunization with SRBCs. Each bar represents an individual mouse; numbers in top right corners indicate total GC cells per spleen ($\times 10^6$) in each group of mice (mean and s.d.). Data are from three independent experiments.

In contrast, DOCK8 deficiency more profoundly disrupted the response 4.5–10 d after immunization, when wild-type SW_{HEL} B cells undergo hypermutation and affinity maturation. Although there was no discernable difference in their location in GCs on days 4.5 and 5 after immunization (**Fig. 6a** and **Supplementary Fig. 5**), the accumulation of SW_{HEL} *pri/pri* GC cells was one third that of wild-type control cells at this time (**Figs. 5b** and **6b**) and fell to one fortieth that of controls by day 9 despite ongoing GCs composed of wild-type host B cells and T cells (**Fig. 6b**). We also observed this difference after adoptive transfer of lymph node cells from SW_{HEL} mice (**Supplementary Fig. 6**), which excluded the possibility that it resulted from the absence of MZB cells among transferred *pri/pri* SW_{HEL} spleen cells. IgG1-switched B cells doubled as a percentage of wild-type SW_{HEL} B cells on day 9 compared with the percentage at day 7 or 5, whereas the percentage IgG1$^+$ failed to increase in SW_{HEL} GC B cells bearing the *pri* mutation (**Fig. 6b**).

Nine days after immunization with HEL^{2X} SRBCs, sequencing of *Igh* in individual flow cytometry–sorted SW_{HEL} GC B cells showed that wild-type cells had accumulated a high ratio of replacement to silent mutations (10.3) in sequences encoding the CDR2 residues contacting the D101R substitution in HEL^{2X} (**Fig. 6c**,**d** and **Supplementary Fig. 7**). Six of the thirty-eight cells analyzed (16%) had Y58F replacements in CDR2 that have been shown to increase affinity[24]. Flow cytometry staining with nanomolar concentrations of the HEL^{3X} antigen allowed us to directly count high-affinity IgG$^+$ variants for D101R-substituted HEL at this time, which comprised 18% of wild-type IgG$^+$ SW_{HEL} B cells, 3.4% of all SW_{HEL} B cells and 0.0082% of all spleen cells (**Fig. 6e**). Sorted *pri/pri* GC cells on day 9 had accumulated the same or a greater load of V_H nucleotide mutations (a mean of 2.3 per cell) compared with that of their wild-type counterparts (a mean of 2.0), including similar numbers of mutations in the CDR2 codons. Despite undergoing comparable hypermutation, the mutant GC cells had a low ratio of replacement to silent mutations in CDR2 (2.4), and only 2 of 44 cells (4.5%) had Y58F replacements (**Fig. 6d** and **Supplementary Fig. 7**). Flow cytometry staining with HEL^{3X} showed that *pri/pri* SW_{HEL} B cells generated few high-affinity IgG$^+$ variants to D101R-substituted HEL even after adjustment for their poor survival (**Fig. 6e**). These cells represented only 3% of IgG1$^+$ SW_{HEL} B cells, 0.2% of the SW_{HEL} B cells and 0.00004% of all spleen cells. DOCK8 deficiency thus allows normal immunoglobulin gene hypermutation but diminishes survival and selection so that the formation of higher-affinity IgG$^+$ B cells was only 0.5% of normal.

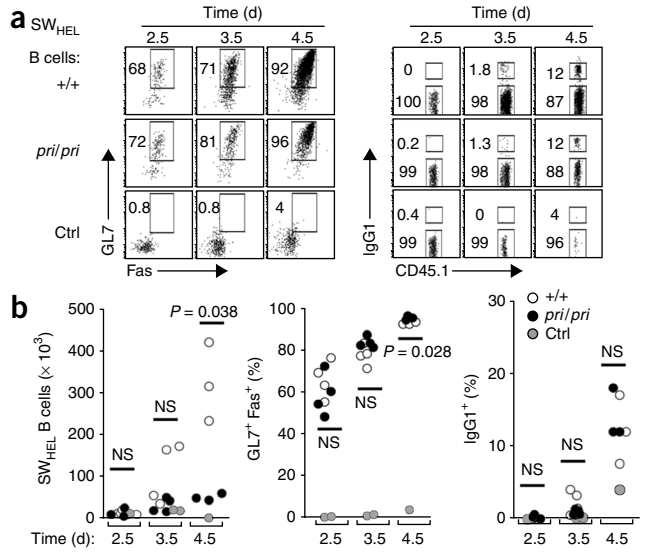

Figure 5 DOCK8-mutant B cells undergo normal T cell–dependent activation, switching and initial differentiation into GC cells *in vivo*. (**a**) Flow cytometry of spleen cells from wild-type mice given adoptive transfer of HEL-specific wild-type or *pri/pri* B cells from SW_{HEL}-transgenic mice (allotypically tagged by CD45.1), then immunized with HEL^{2X}-SRBCs (above plots, time after transfer and immunization). Plots are gated on HEL$^+$CD45.1$^+$B220$^+$ SW_{HEL} B cells; numbers adjacent to outlined areas indicate percent GL7$^+$Fas$^+$ cells (left) and IgG1$^+$ switched cells (right, top) and unswitched cells (right, bottom). Ctrl, control mice given SW_{HEL} B cells but immunized with unconjugated SRBCs lacking HEL. (**b**) HEL$^+$CD45.1$^+$B220$^+$ SW_{HEL} B cells (left) from the recipient mice in **a** at various times after immunization (horizontal axes), and frequency of SW_{HEL} B cells that were GL7$^+$Fas$^+$ (middle) or switched to IgG1 (right). Each symbol represents an individual mouse; small horizontal lines indicate the mean. *P* values, wild-type versus *pri/pri* (unpaired *t*-test with Welch's correction). Data are representative of an experiment done once.

Defective B cell synapses

Systematic analysis of the effects of DOCK8 deficiency on established molecular pathways for the formation of GC and MZB cells showed selective disruption of immunological synapse organization. When B cells recognize antigen on cell membranes, BCR signaling triggers

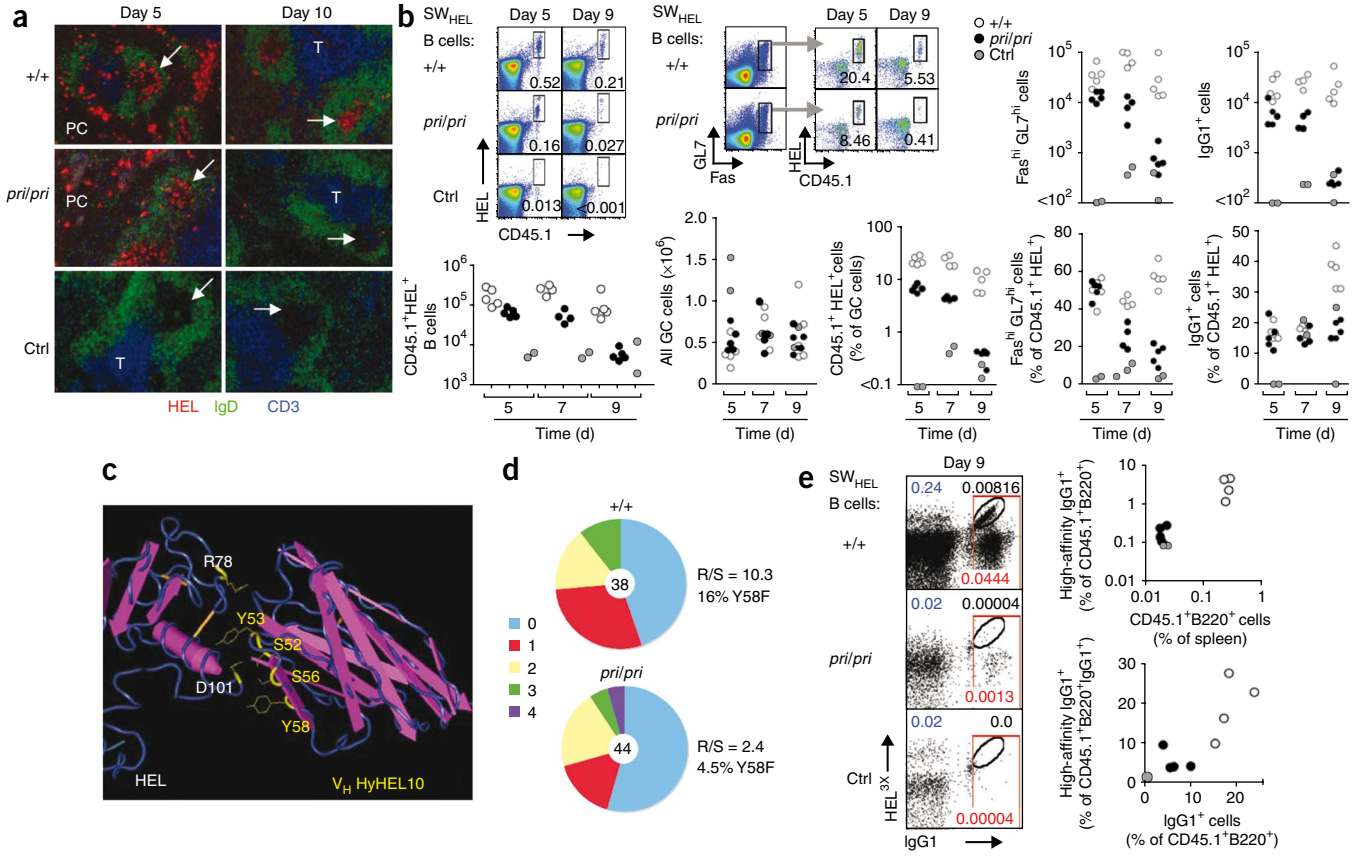

Figure 6 Intrinsic failure of DOCK8-mutant GC B cells to persist or undergo affinity maturation. (**a**) Confocal immunofluorescence of spleen cryosections from wild-type B6 mice injected with HEL-specific wild-type or *pri/pri* B cells from SW_{HEL}-transgenic mice (allotypically tagged as CD45.1), then immunized with HEL^{2X} SRBCs and assessed 5 or 10 d later by staining for HEL, IgD and CD3. PC, extrafollicular plasma cell foci; T, T cell zones; arrows indicate GCs. Original magnification, ×10. (**b**) Flow cytometry (top left) and number or frequency (bottom and right) of $CD45.1^+$ HEL-binding B cells and GC cells derived from wild-type or *pri/pri* $HEL^+CD45.1^+$ SW_{HEL} cells 5–9 d after adoptive transfer (as in **a**), as well as total GC B cells per spleen, frequency of GC B cells that were SW_{HEL} B cells, and frequency and absolute number of $HEL^+CD45.1^+$ SW_{HEL} $FAS^{hi}HEL^{lo}$ GC cells and IgG1-switched cells. $P = 0.008$, percent GC B cells that were SW_{HEL} B cells on day 9, +/+ versus *pri/pri* (Student's *t*-test with Welch's correction). (**c**) Structure of HEL in complex with the SW_{HEL} antibody HyHEL10, showing the position of the two HEL residues that are mutant in HEL^{2X} and four of the D101 contact residues in the heavy-chain CDR2. (**d**) Sequencing analysis of heavy-chain genes from +/+ or *pri/pri* SW_{HEL} GC B cells sorted by flow cytometry. Left, proportion of cells containing 0–4 mutations (key) in the sequence encoding CDR2; center, total number of cells sequenced. Right, replacement/silent ratio (R/S) and percent cells with the Y58F replacement substitution. (**e**) High-affinity variants on day 9 after immunization (as in **a**) assessed by direct assay for binding to nanomolar concentrations of the D101R mutant HEL^{3X}. Left, flow cytometry gated on $B220^+CD45.1^+$ SW_{HEL} B cells, from data collected on 11×10^6 to 22×10^6 spleen cells combined from four individual recipients of wild-type or *pri/pri* SW_{HEL} B cells or from two recipients immunized with uncoupled SRBCs. Numbers in plots indicate percent spleen cells that are $CD45.1^+$ SW_{HEL} B cells (blue) or switched to IgG1 (red), or mutated B cells with BCRs of higher affinity (oval gate; black numbers above indicate percent spleen cells in this gate). Right, data for individual mice. $P < 0.05$, *pri/pri* and +/+ SW_{HEL} high-affinity cells among $CD45.1^+B220^+$ cells ($P = 0.038$) or $CD45.1^+B220^+IgG1^+$ cells ($P = 0.031$) remaining on day 9 (Student's *t*-test with Welch's correction). Ctrl (**a**,**b**,**e**), control mice given SW_{HEL} B cells but immunized with unconjugated SRBCs lacking HEL. Each symbol represents an individual mouse (**b**,**e**). Data are representative of four independent experiments (**a**–**c**) or one experiment each for **d**,**e** (independent of each other).

the integrin LFA-1 to bind strongly to its ligand ICAM-1 (A002871) on the antigen-presenting membrane, which promotes strong B cell adhesion and spreading[25]. During the first 3 min of this process, BCRs become polarized in the center of the adhesion zone and cluster antigen into a central supramolecular cluster. LFA-1 becomes polarized into a surrounding peripheral supramolecular cluster, where it concentrates ICAM-1 in the antigen-presenting membrane. We isolated DOCK8-mutant and wild-type B cells from MD4-transgenic mice expressing HEL-specific BCRs. We allowed the B cells to settle on planar membranes containing fluorescence-tagged HEL antigen and ICAM-1 and imaged them by a combination of confocal, differential interference contrast and interference-reflection microscopy. Both mutant and wild-type cells adhered and clustered antigen into a central supramolecular cluster, but the mutant cells showed an inability to cluster ICAM-1 into a peripheral supramolecular cluster and consequently formed smaller areas of close membrane apposition (**Fig. 7a**).

In contrast to its effect on the disruption of B cell synapse formation, *Dock8* mutation had no effect on other BCR signaling events, including an increase in intracellular calcium stimulated by antibody to IgM (anti-IgM; **Fig. 7b**) or phosphorylation of the kinase Erk (data not shown), induction of the activation markers CD25, CD86 and CD69 (**Fig. 7c** and data not shown), or induction of DNA synthesis (**Supplementary Fig. 8**) or cell division (**Fig. 7d**), even in conditions of limiting BCR engagement (**Fig. 7d** and **Supplementary Figs. 9** and **10**). The mutation also had no discernable effect on CD40- or lipopolysaccharide-stimulated activation or proliferation (**Fig. 7d**, **Supplementary Figs. 8–10** and data not shown). DOCK8-mutant B cells were also normal in forming stable conjugates during antigen presentation to specific $CD4^+$

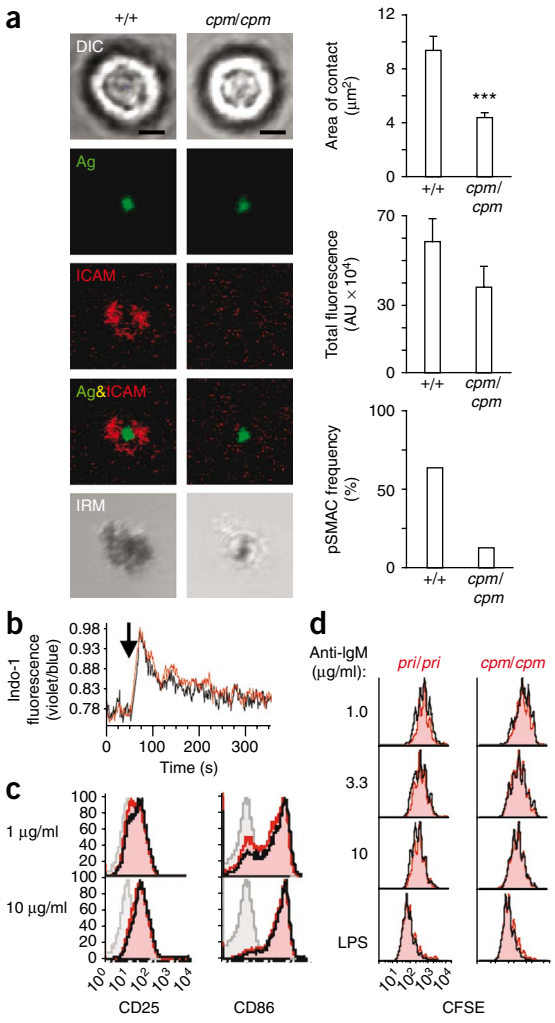

Figure 7 *Dock8* mutations disrupt the formation of the B cell immunological synapse but not other aspects of signaling through the B cell antigen receptor. (**a**) Differential interference contrast microscopy (DIC), confocal fluorescence microscopy (middle three images) and interference reflection microscopy (IRM) of HEL-specific MD4 wild-type or mutant B cells allowed to settle onto lipid bilayers containing monobiotinylated HEL antigen (Ag; green) and Alexa Fluor 532–conjugated ICAM-1 (ICAM; red) and imaged after 10 min of interaction. Scale bar, 2 μm. Right, area of B cell contact with the bilayer (top), antigen accumulation at the contact site (middle; presented in arbitrary units (AU)), and frequency of B cells forming a peripheral ring of ICAM-1 (pSMAC; bottom). Results are representative of three independent experiments (mean and s.e.m.). (**b**) Change in intracellular calcium concentration in mixtures of *pri/pri* CD45.2$^+$ spleen cells (red line) and wild-type CD45.1$^+$ spleen cells (black line) stimulated with anti-IgM (downward arrow), presented as the ratio of violet to blue Indo-1 fluorescence. (**c**) Expression of CD25 and CD86 on wild-type (black lines) or *pri/pri* (red filled histograms) lymph node B cells left unstimulated (grey filled histograms) or 18 h after stimulation with anti-IgM (1 or 10 μg/ml). Data are representative of one experiment with four mice per group. (**d**) Division of lymph node B cells, measured as dilution of the cytosolic dye CFSE in B220$^+$7AAD$^-$ cells after 4 d of culture with anti-IgM or lipopolysaccharide (LPS). Mutant *pri/pri* or *cpm/cpm* CD45.2$^+$ cells (red filled histograms) labeled with CFSE were cultured with wild-type CD45.1$^+$ cells (black lines) in the same wells to control for experimental variation. Data are representative of three experiments presenting six of eight independent samples assessed (two samples showed slightly less CFSE dilution by *pri/pri* cells; **Supplementary Fig. 9**).

T cells, in a B cell–T cell adhesion process that depends on the adaptor protein SAP in T cells and is important for GC formation[26] (**Supplementary Fig. 11**). *Dock8* mutation also did not decrease the *in vivo* homing and accumulation of B cells in lymph nodes in mixed chimeras (**Supplementary Fig. 12**), despite the dependency of this process on CCR7 and CXCR4 chemokine receptor signaling of the adhesion of LFA-1 to ICAM-1 (ref. 27). After adoptive transfer, DOCK8-mutant SW_{HEL} B cells migrated and positioned themselves normally in follicles and GCs (**Fig. 6a** and **Supplementary Fig. 5**). Mutant and wild-type spleen B cells were indistinguishable by *in vitro* chemotaxis to the three main chemotactic factors for B cells: S1P, CXCL12 and CXCL13 (**Supplementary Fig. 13**). DOCK8 therefore functions quite specifically in B cells, being necessary for BCR signaling of integrin–ICAM-1 polarization in the immunological synapse but not for many other BCR-mediated, chemotactic or integrin-mediated processes.

DISCUSSION

The findings presented here have shown that mutations in *Dock8* caused humoral immunodeficiency that preserved T cell–independent antibody formation and the initial extrafollicular wave of T cell–dependent antibody formation but severely crippled the longevity and affinity maturation of T cell–dependent antibody responses. The basis for these humoral deficits was a profound defect in the survival and selection of GC B cells during the affinity-maturation phase of GC responses, due to an intrinsic requirement for DOCK8 in the GC B cells themselves. The GC B cell defect may have been compounded by the lower number of CD4$^+$ helper T cells in DOCK8-mutant mice, although mixed-chimera and adoptive-transfer studies clearly established that the mutation profoundly crippled the persistence and affinity maturation of mutant GC B cells even in the presence of a normal complement of helper T cells. In B cells, DOCK8 has a critical role in antigen recognition, being essential for the recruitment of ICAM-1 to the immunological synapse but unnecessary for the central events in BCR signaling to soluble ligands that lead to activation and proliferation. The requirement for DOCK8 in B cell synapse formation and for longevity and affinity maturation of T cell–dependent antibody elucidates an important step in the establishment of humoral immunity.

The requirement for DOCK8 in the organization of a normally polarized B cell immunological synapse is very similar to defects in B cell formation of peripheral supramolecular clusters caused by mutations in the genes encoding the Rho-family G protein Rac2 (A002002) or the Rac guanine-exchange factors Vav1 and Vav2 (A002361)[28]. Compared with those proteins, DOCK8 seems to have a more restricted function for BCR-integrin coordination, because follicular B cell development, migration, chemotaxis, activation and T cell–independent type 2 antibody responses were normal in DOCK8-mutant B cells, whereas pleiotropic defects in these processes are caused by mutations in genes encoding Rac2 or Vav proteins. In addition to their role in BCR-integrin coordination, Rac2 and Vav proteins are critical for the initial events in BCR signaling of intracellular calcium and proliferation in response to soluble anti-IgM and for chemokine responsiveness[29–32]. The specificity of DOCK8 function in BCR-integrin signaling and GC selection in B cells also contrasts with that of DOCK2, whose gene mutation in mice causes profound lymphopenia, disrupted lymphoid architecture, crippled B cell migration to lymph nodes and to CXCL12 and CXCL13 chemokines *in vitro*[33] and a generalized defect in B cell integrin activation in response to a range of stimuli[34]. To understand how DOCK8 serves such a restricted role in B cells compared with that of Rac2, Vav or

DOCK2, it will be worthwhile in future work to define the G proteins and biochemical pathway regulated by DOCK8 for the formation of B cell immunological synapses.

Mutations in *CD19*, which encodes a coreceptor that is phosphorylated by BCR engagement and then recruits PI(3)K[5], cause a human CVID syndrome with normal numbers of IgD^+ recirculating B cells and presence of GCs but low numbers of $CD27^+$ memory B cells and low-avidity antibody to rabies vaccine[4]. In the mouse, *Cd19* mutations that eliminate the protein or inactivate its ability to recruit PI(3)K cause a humoral immunodeficiency syndrome that closely resembles that caused by *Dock8* mutation. These mice have normal numbers of recirculating IgD^+ B cells, lack of MZB cells, a normal calcium response and proliferation in response to stimulation with soluble anti-IgM, relatively normal TI-2 antibody responses, and initiation of GC reactions and isotype switching but limited expansion of GCs and failure of affinity maturation or long-lived antibody[35–38]. The smaller GC size and loss of MZB cells in CD19 mutant mice can be 'rescued' by a mutation in *Pten* (encoding PtdIns(3,4,5)P_3 phosphatase), which emphasizes the involvement of PtdIns(3,4,5)P_3 lipid products of PI(3)K in these processes[39]. A distinction between mutations in the genes encoding CD19 and DOCK8 is that CD19 deficiency greatly diminished the early step of B cell adhesion and clustering of membrane HEL antigen in the bilayer assay used here[40], whereas DOCK8 deficiency was restricted to disruption of the later step of peripheral supramolecular cluster formation. This difference may reflect the proximal role of CD19 in recruiting not only PI(3)K but also BCR signaling molecules with general involvement in the initiation of BCR signaling, such as Lyn[41]. The phenotypic similarities and the fact that the DHR1 domain of related DOCK proteins binds PtdIns(3,4,5)P_3 lipids to recruit these guanine-exchange factors to the membrane and activate Rac at sites of PI(3)K activation[13] make it logical to hypothesize that DOCK8 serves as an effector downstream of CD19 and PI(3)K to promote G protein signaling events critical for integrin polarization at the synapse and for the survival of MZB cells and GC B cells.

The discovery here that *Dock8* mutations resulted in humoral immune deficiency in mice is complemented by the independent discovery of *DOCK8* mutations associated with immunodeficiency in humans[42]. Recurrent sinopulmonary bacterial infections typical of humoral immunodeficiency have been observed in DOCK8-deficient people, in addition to cutaneous viral infections usually associated with partial T cell deficiency. Despite having normal or increased concentrations of serum IgG, these people show a variable lack of antibody to T cell–dependent vaccines. Our data here have established that DOCK8 deficiency indeed causes a primary humoral immunodeficiency that selectively affects the longevity and maturation of T cell–dependent antibody responses to protein antigens and have established its cellular basis and its B cell–intrinsic role. Although the focus of our study here was to understand the humoral defects caused by DOCK8 deficiency, an additional requirement for DOCK8 in T cells has been demonstrated here and associated with the human syndrome. Future, separate studies will be needed to define the cellular basis for the lower numbers of peripheral T cells caused by *Dock8* mutation.

The requirement for DOCK8 in the formation of MZB cells may be explained by the fact that this B cell subset is highly dependent on both BCR-CD19-PI(3)K signaling[35,38,43–45] and integrin signaling[46,47]. Coordinated signaling by BCR and integrins has also been proposed as being critical for GC B cell survival and selection, as ICAM-1 has high expression on follicular dendritic cells (FDCs) presenting antigen in GCs and inhibits apoptosis of GC B cells *in vitro*[48]. ICAM-1 is not induced on FDCs when the gene encoding the kinase IKKβ is selectively inactivated in these cells, and this leads to small GCs[49]. *In vivo* soluble antigen has the opposite effect from FDC–bound antigen on GC B cells by triggering apoptosis within 4 h (refs. 50,51). Costimulation with ICAM-1 has also been shown to modify the outcome of TCR stimulation in ways that are distinct from costimulation with CD28, converting a death signal into a survival signal in immature thymocytes[52,53] and being critical in formation of memory $CD8^+$ T cells[54]. We speculate that DOCK8 immunodeficiency may result from the failure of GC B lymphocytes and some classes of T cells to organize a normal immunological synapse and thereby receive an integrin costimulus during antigen recognition that is needed to convert an antigen receptor–induced death signal into a survival signal.

METHODS

Methods and any associated references are available in the online version of the paper at http://www.nature.com/natureimmunology/.

Accession codes. UCSD-Nature Signaling Gateway (http://www.signaling-gateway.org): A000538, A001770, A002062, A002871, A002002 and A002361.

Note: Supplementary information is available on the Nature Immunology website.

ACKNOWLEDGMENTS

We thank M. Townsend, D. Howard, H. Ferry and C. Gillespie for technical assistance; the staff of the Australian National University Bioscience Division and Oxford Biomedical Services Unit for animal husbandry; the Australian Phenomics Facility genotyping and mapping team for genetic analysis, R. Rigby, B. Balakishnan and L. Beaton (Australian National University) for advice and reagents; J. Cannons and P. Schwartzberg (National Institutes of Health) for B cell–T cell conjugation methods and SAP-deficient mice; C. Jenne, S. Watson and T. Pham (University of California, San Francisco) for collaboration; R. Schwartz (National Institutes of Health) for support with advice and reagents; and H. Su (National Institutes of Health) for sharing findings about human DOCK8 deficiency before publication. Supported by the Wellcome Trust (R.J.C. and C.C.G.), the Australian Research Council (C.C.G.), the National Health and Medical Research Council (C.C.G., R.B., S.G.T., C.G.V., F.M., K.L.R., L.E.T. and E.K.D.), the Medical Research Council (T.L. and R.J.C.), The Ramaciotti Foundation (A.E. and C.C.G.), Deutsche Forschungsgemeinschaft (A.E.), Cancer Research UK (F.D.B.), the Andrew McMichael Trust Fund (R.J.C.) and the National Institute for Health Research Biomedical Research Centre Programme (R.J.C.).

AUTHOR CONTRIBUTIONS

T.L., K.L.R., A.J., T.B.-J. and B.W. mapped and identified the mutations; K.L.R. analyzed *pri* and complementation crosses with E.K., H.D., L.E.T. and A.E.; T.L. analyzed *cpm* with T.L.C., A.J., T.B.-J., D.A. and J.G.C.; B.T. and F.D.B. did synapse analysis; M.J.L. supervised early experiments on *cpm* by A.J.; F.M. and K.L.R. analyzed the effects of the BAFF transgene; E.K.D. and S.G.T. analyzed SAP-dependent B cell–T cell conjugation; K.L.R., T.D.C., T.C. and R.B. analyzed GC response in the SW_{HEL} adoptive-transfer system; C.G.V. and E.K. designed and established the genetic screen and identified *cpm* and *pri* founders; C.C.G. and R.J.C. initiated and contributed to all aspects of study design and interpretation; and K.L.R., T.L., R.J.C. and C.C.G. wrote the paper in consultation with all coauthors.

Published online at http://www.nature.com/natureimmunology/.
Reprints and permissions information is available online at http://npg.nature.com/reprintsandpermissions/.

1. Conley, M.E. *et al.* Primary B cell immunodeficiencies: comparisons and contrasts. *Annu. Rev. Immunol.* **27**, 199–227 (2009).
2. Park, M.A., Li, J.T., Hagan, J.B., Maddox, D.E. & Abraham, R.S. Common variable immunodeficiency: a new look at an old disease. *Lancet* **372**, 489–502 (2008).
3. Schaffer, A.A., Salzer, U., Hammarstrom, L. & Grimbacher, B. Deconstructing common variable immunodeficiency by genetic analysis. *Curr. Opin. Genet. Dev.* **17**, 201–212 (2007).
4. van Zelm, M.C. *et al.* An antibody-deficiency syndrome due to mutations in the CD19 gene. *N. Engl. J. Med.* **354**, 1901–1912 (2006).

5. Tuveson, D.A., Carter, R.H., Soltoff, S.P. & Fearon, D.T. CD19 of B cells as a surrogate kinase insert region to bind phosphatidylinositol 3-kinase. *Science* **260**, 986–989 (1993).
6. Castigli, E. *et al.* TACI is mutant in common variable immunodeficiency and IgA deficiency. *Nat. Genet.* **37**, 829–834 (2005).
7. Salzer, U. *et al.* Mutations in TNFRSF13B encoding TACI are associated with common variable immunodeficiency in humans. *Nat. Genet.* **37**, 820–828 (2005).
8. Grimbacher, B. *et al.* Homozygous loss of ICOS is associated with adult-onset common variable immunodeficiency. *Nat. Immunol.* **4**, 261–268 (2003).
9. Wehr, C. *et al.* The EUROclass trial: defining subgroups in common variable immunodeficiency. *Blood* **111**, 77–85 (2008).
10. MacLennan, I.C.M. *et al.* Extrafollicular antibody responses. *Immunol. Rev.* **194**, 8–18 (2003).
11. Hande, S., Notidis, E. & Manser, T. Bcl-2 obstructs negative selection of autoreactive, hypermutated antibody V regions during memory B cell development. *Immunity* **8**, 189–198 (1998).
12. Naparstek, Y. *et al.* A single germline VH gene segment of normal A/J mice encodes autoantibodies characteristic of systemic lupus erythematosus. *J. Exp. Med.* **164**, 614–626 (1986).
13. Cote, J.-F. & Vuori, K. GEF what? Dock180 and related proteins help Rac to polarize cells in new ways. *Trends Cell Biol.* **17**, 383–393 (2007).
14. Meller, N., Merlot, S. & Guda, C. CZH proteins: a new family of Rho-GEFs. *J. Cell Sci.* **118**, 4937–4946 (2005).
15. Ruusala, A. & Aspenstrom, P. Isolation and characterisation of DOCK8, a member of the DOCK180-related regulators of cell morphology. *FEBS Lett.* **572**, 159–166 (2004).
16. Yang, J., Zhang, Z., Roe, S.M., Marshall, C.J. & Barford, D. Activation of Rho GTPases by DOCK exchange factors is mediated by a nucleotide sensor. *Science* **325**, 1398–1402 (2009).
17. Phan, T.G. *et al.* B cell receptor-independent stimuli trigger immunoglobulin (Ig) class switch recombination and production of IgG autoantibodies by anergic self-reactive B cells. *J. Exp. Med.* **197**, 845–860 (2003).
18. Paus, D. *et al.* Antigen recognition strength regulates the choice between extrafollicular plasma cell and germinal center B cell differentiation. *J. Exp. Med.* **203**, 1081–1091 (2006).
19. Phan, T.G. *et al.* High affinity germinal center B cells are actively selected into the plasma cell compartment. *J. Exp. Med.* **203**, 2419–2424 (2006).
20. Kam-Morgan, L.N. *et al.* High-resolution mapping of the HyHEL-10 epitope of chicken lysozyme by site-directed mutagenesis. *Proc. Natl. Acad. Sci. USA* **90**, 3958–3962 (1993).
21. Padlan, E.A. *et al.* Structure of an antibody-antigen complex: crystal structure of the HyHEL-10 Fab-lysozyme complex. *Proc. Natl. Acad. Sci. USA* **86**, 5938–5942 (1989).
22. Hasbold, J., Corcoran, L.M., Tarlinton, D.M., Tangye, S.G. & Hodgkin, P.D. Evidence from the generation of immunoglobulin G-secreting cells that stochastic mechanisms regulate lymphocyte differentiation. *Nat. Immunol.* **5**, 55–63 (2004).
23. Chan, T.D. *et al.* Antigen affinity controls rapid T-dependent antibody production by driving the expansion rather than the differentiation or extrafollicular migration of early plasmablasts. *J. Immunol.* **183**, 3139–3149 (2009).
24. Li, Y., Li, H., Yang, F., Smith-Gill, S.J. & Mariuzza, R.A. X-ray snapshots of the maturation of an antibody response to a protein antigen. *Nat. Struct. Biol.* **10**, 482–488 (2003).
25. Carrasco, Y.R., Fleire, S.J., Cameron, T., Dustin, M.L. & Batista, F.D. LFA-1/ICAM-1 interaction lowers the threshold of B cell activation by facilitating B cell adhesion and synapse formation. *Immunity* **20**, 589–599 (2004).
26. Qi, H., Cannons, J.L., Klauschen, F., Schwartzberg, P.L. & Germain, R.N. SAP-controlled T-B cell interactions underlie germinal centre formation. *Nature* **455**, 764–769 (2008).
27. Okada, T. *et al.* Chemokine requirements for B cell entry to lymph nodes and Peyer's patches. *J. Exp. Med.* **196**, 65–75 (2002).
28. Arana, E. *et al.* Activation of the small GTPase Rac2 via the B cell receptor regulates B cell adhesion and immunological-synapse formation. *Immunity* **28**, 88–99 (2008).
29. Croker, B.A. *et al.* The Rac2 guanosine triphosphatase regulates B lymphocyte antigen receptor responses and chemotaxis and is required for establishment of B-1a and marginal zone B lymphocytes. *J. Immunol.* **168**, 3376–3386 (2002).
30. Doody, G.M. *et al.* Signal transduction through Vav-2 participates in humoral immune responses and B cell maturation. *Nat. Immunol.* **2**, 542–547 (2001).
31. Tedford, K. *et al.* Compensation between Vav-1 and Vav-2 in B cell development and antigen receptor signaling. *Nat. Immunol.* **2**, 548–555 (2001).
32. Walmsley, M.J. *et al.* Critical roles for Rac1 and Rac2 GTPases in B cell development and signaling. *Science* **302**, 459–462 (2003).
33. Fukui, Y. *et al.* Haematopoietic cell-specific CDM family protein DOCK2 is essential for lymphocyte migration. *Nature* **412**, 826–831 (2001).
34. Nombela-Arrieta, C. *et al.* Differential requirements for DOCK2 and phosphoinositide-3-kinase γ during T and B lymphocyte homing. *Immunity* **21**, 429–441 (2004).
35. Wang, Y. *et al.* The physiologic role of CD19 cytoplasmic tyrosines. *Immunity* **17**, 501–514 (2002).
36. Rickert, R.C., Rajewsky, K. & Roes, J. Impairment of T-cell-dependent B-cell responses and B-1 cell development in CD19-deficient mice. *Nature* **376**, 352–355 (1995).
37. Engel, P. *et al.* Abnormal B lymphocyte development, activation, and differentiation in mice that lack or overexpress the CD19 signal transduction molecule. *Immunity* **3**, 39–50 (1995).
38. Wang, Y. & Carter, R.H. CD19 regulates B cell maturation, proliferation, and positive selection in the FDC zone of murine splenic germinal centers. *Immunity* **22**, 749–761 (2005).
39. Anzelon, A.N., Wu, H. & Rickert, R.C. Pten inactivation alters peripheral B lymphocyte fate and reconstitutes CD19 function. *Nat. Immunol.* **4**, 287–294 (2003).
40. Depoil, D. *et al.* CD19 is essential for B cell activation by promoting B cell receptor-antigen microcluster formation in response to membrane-bound ligand. *Nat. Immunol.* **9**, 63–72 (2008).
41. Fujimoto, M. *et al.* CD19 regulates Src family protein tyrosine kinase activation in B lymphocytes through processive amplification. *Immunity* **13**, 47–57 (2000).
42. Zhang, Q. *et al.* Combined immunodeficiency associated with DOCK8 mutations. *N. Engl. J. Med.* published online doi:10.1056/NEJMoa0905506 (23 September 2009).
43. Martin, F. & Kearney, J.F. Positive selection from newly formed to marginal zone B cells depends on the rate of clonal production, CD19, and btk. *Immunity* **12**, 39–49 (2000).
44. Okkenhaug, K. *et al.* Impaired B and T cell antigen receptor signaling in p110δ PI 3-kinase mutant mice. *Science* **297**, 1031–1034 (2002).
45. Clayton, E. *et al.* A crucial role for the p110δ subunit of phosphatidylinositol 3-kinase in B cell development and activation. *J. Exp. Med.* **196**, 753–763 (2002).
46. Lu, T.T. & Cyster, J.G. Integrin-mediated long-term B cell retention in the splenic marginal zone. *Science* **297**, 409–412 (2002).
47. Guinamard, R., Okigaki, M., Schlessinger, J. & Ravetch, J.V. Absence of marginal zone B cells in Pyk-2-deficient mice defines their role in the humoral response. *Nat. Immunol.* **1**, 31–36 (2000).
48. Koopman, G. *et al.* Adhesion through the LFA-1 (CD11a/CD18)-ICAM-1 (CD54) and the VLA-4 (CD49d)-VCAM-1 (CD106) pathways prevents apoptosis of germinal center B cells. *J. Immunol.* **152**, 3760–3767 (1994).
49. Victoratos, P. *et al.* FDC-specific functions of p55TNFR and IKK2 in the development of FDC networks and of antibody responses. *Immunity* **24**, 65–77 (2006).
50. Pulendran, B., Kannourakis, G., Nouri, S., Smith, K.G. & Nossal, G.J. Soluble antigen can cause enhanced apoptosis of germinal-centre B cells. *Nature* **375**, 331–334 (1995).
51. Shokat, K.M. & Goodnow, C.C. Antigen-induced B-cell death and elimination during germinal-centre immune responses. *Nature* **375**, 334–338 (1995).
52. Lucas, B. & Germain, R.N. Opening a window on thymic positive selection: developmental changes in the influence of cosignaling by integrins and CD28 on selection events induced by TCR engagement. *J. Immunol.* **165**, 1889–1895 (2000).
53. Kishimoto, H. *et al.* Differing roles for B7 and intercellular adhesion molecule-1 in negative selection of thymocytes. *J. Exp. Med.* **184**, 531–537 (1996).
54. Scholer, A., Hugues, S., Boissonnas, A., Fetler, L. & Amigorena, S. Intercellular adhesion molecule-1-dependent stable interactions between T cells and dendritic cells determine $CD8^+$ T cell memory. *Immunity* **28**, 258–270 (2008).

ONLINE METHODS

Mice and procedures. All experiments were approved by the Animal Ethics and Experimentation Committee of Australian National University or the Oxford University Ethical Review Committee and were done under UK Home Office License. *N*-ethyl-*N*-nitrosourea (100 mg per kg body weight) was given intraperitoneally to male C57BL/6 mice three times at an interval of 1 week. For bone marrow chimeras, B6.SJL CD45.1$^+$ mice were irradiated with 10 Gy and were injected with 2×10^6 bone marrow cells (50:50 mixture of wild-type B6.SJL CD45.1$^+$ bone marrow and either mutant or wild-type B6 (CD45.2$^+$) marrow). They were allowed to reconstitute for 8–10 weeks before immunization and analysis.

Immunization and enzyme-linked immunosorbent assay. Primary immunization was 50 μg ARS-CGG (Biosearch) and 1×10^8 heat- and formalin-inactivated *B. pertussis* bacteria (Lee Laboratories), precipitated together in alum and PBS and given intraperitoneally to each mouse divided into two 150-μl injections to minimize false-negative reactions. Booster intraperitoneal immunizations were 50 μg ARS-CGG and 25 μg nitrophenyl-Ficoll (Biosearch) in 300 μl PBS. Antibodies were measured by enzyme-linked immunosorbent assay on plates coated with BSA-ARS, CGG (Jackson ImmunoResearch), BSA-nitrophenyl or sonicated *B. pertussis* and were detected with IgG subtype–specific antibodies (IgG1 (1070-04; Southern Biotech) and IgG2a^b (5.7; BD Pharmingen)) or IgM antibody (1021-04; Southern Biotech). For SRBC immunization, mice were given intraperitoneal injection of 200 μl SRBCs (Alsevers) diluted 1.5 times in PBS. Conjugation of SRBCs, adoptive transfer of spleen cells containing 1×10^5 SW_{HEL} B cells per mouse, and immunization with conjugated SRBCs were as described[19].

Flow cytometry. The following antibodies were used (from BD Pharmingen unless stated otherwise): peridinin chlorophyll protein (PerCP)–cyanine 5.5–conjugated anti-CD4 (RM 4.5), phycoerythrin (PE)-conjugated anti-CD5 (53-7.3), PerCP-conjugated anti-CD5 (53-7.3), fluorescein isothiocyanate (FITC)-conjugated anti-CD11b (M1/70), PE–indotricarbocyanine (Cy7)–conjugated anti-CD19 (eBio1D3; eBioscience), FITC-conjugated anti-CD21/35 (7G6), PE-conjugated anti-CD23 (B3B4), PE-Cy7–conjugated anti-CD23 (B3B4; eBioscience), FITC-conjugated anti-CD25 (7D4), PE-conjugated anti-CD38 (90), biotin-conjugated anti-CD45.1 (A20), FITC-conjugated anti-CD45.1 (A20), Alexa Fluor 700–conjugated anti-CD45.1 (A20; Biolegend), Pacific blue–conjugated anti-CD45.2 (104; Biolegend), PE-conjugated anti-CD69 (H1.2F3), allophycocyanin-conjugated anti-CD86 (GL1), PE-conjugated anti-CD86 (GL1), allophycocyanin-conjugated anti-CD93 (AA4.1; eBioscience), PE-conjugated anti-CD95 (Jo-2), FITC-conjugated anti-B220 (RA3-6B2), PerCP-conjugated anti-B220 (RA3-6B2), PerCP–cyanine 5.5–conjugated anti-B220 (RA3-6B2), allophycocyanin–Alexa Fluor 750–conjugated anti-B220 (RA3-6B2; Caltag), PE-Cy7–conjugated anti-B220 (RA3-6B2; eBioscience), allophycocyanin-conjugated IgM (II/41), biotin-conjugated IgM (II/41), PE-conjugated IgD (11–26; Southern Biotech), FITC-conjugated IgD (11–26), PE-conjugated IgG1 (A85-1), FITC-conjugated antibody to B and T cell antigen (GL7), streptavidin–PerCP–cyanine 5.5, streptavidin-PE-Cy7 (eBioscience), streptavidin-allophycocyanin-Cy7, and HyHEL9 conjugated to Alexa Fluor 647 with a Monoclonal Antibody Labeling kit (Molecular Probes). Staining with HyHEL9 followed incubation with HEL (Sigma) or HEL^{3X} at a concentration of 50 ng/ml. Data were acquired on a FACSCanto, FACSCalibur, FACSort or LSR II (BD) and were analyzed with FlowJo Software (Tree Star).

SHM analysis. SW_{HEL} GC B cells (B220$^+$CD45.1$^+$CD38$^-$) were sorted from recipient mice 9 d after transfer and immunization with HEL^{2X} SRBCs and were deposited as single cells in 96-well plates; the SW_{HEL} heavy-chain V region was amplified from genomic DNA by nested PCR and products were sequenced without cloning as described[18].

Immunohistochemistry and immunofluorescence. Tissues were snap-frozen in liquid nitrogen and embedded in optimum cutting temperature compound (Tissue-Tek). Sections 5 μm in thickness were cut and air-dried and were fixed for 20 min in ice-cold acetone. Sections were washed in 50 mM Tris-buffered saline, pH 7.6, or PBS between all steps and antibodies were added for incubation of 30–45 min at 25 °C (immunohistochemistry) or 37 °C (immunofluorescence).

Reagents for immunohistochemistry were as follows. For **Figure 4a**, biotin-conjugated anti-PNA (B1075; Vector) and sheep anti–mouse IgD (PC283; Binding Site), peroxidase-conjugated donkey anti–sheep IgG (713-035-147; Jackson ImmunoResearch) and streptavidin–alkaline phosphatase (Vector) were used; peroxidase was detected with 3,3′-diaminobenzedine (Sigma) and hydrogen peroxide, and alkaline phosphatase activity was detected with the Alkaline Phosphatase Substrate III kit (SK 5300; Vector) according to the manufacturer's instructions. For **Figure 2d**, frozen sections were incubated with biotin-conjugated anti-CD1d (1B1; eBioscience) and antibody was detected with an Alkaline Phosphatase Substrate III kit (SK 5300; Vector) followed by rat anti–mouse MAdCAM (MECA-367; Serotec) and biotin-conjugated goat anti–rat IgG (STAR80B; Serotec), detected with Strep ABC/HRP (K0377; Dako) and 3,3′-diaminobenzedine, (SK-4100; Vector). For immunofluorescence, slides were incubated with HEL protein in 5% (vol/vol) mouse serum, then with biotin-conjugated HyHEL5, followed by FITC-conjugated IgD, PE-conjugated anti-CD3 (2C11) and streptavidin-allophycocyanin (all from BD Pharmingen). Images were obtained with an Olympus IX71, Nikon TE2000U or Leica confocal microscope (TCS SP5).

***In vitro* cell stimulation assays.** Intracellular calcium was measured with the calcium indicator Indo-1 (Invitrogen) before and after stimulation with goat anti-IgM F(ab′)$_2$ (50 μg/ml; 115-006-075; Jackson ImmunoResearch) with an LSR I (BD) as described[55]. Proliferation and overnight activation of lymph node lymphocytes was done in RPMI medium supplemented with 10% (vol/vol) FCS, 55 μM β-mercaptoethanol and 50 units per ml of penicillin-streptomycin, and cells were stimulated with goat anti-IgM F(ab′)$_2$ (Jackson ImmunoResearch) at a concentration of 0.33, 1, 3.3 or 10 μg/ml alone and together with anti-CD40 (10 μg/ml; 1C10). DNA synthesis assays were done as described[56]. For cell division assays, cells were labeled for 5 min at 37 °C with 1.5 μM CFSE (carboxyfluorescein diacetate succinimidyl ester) and then were cultured for 96 h. For chemotaxis assays, cells were washed several times in RPMI-1640 medium with 0.5% (wt/vol) fatty acid–free BSA, were resensitized for 30 min at 37 °C and then were tested for 3 h for transmigration across uncoated 5-mm Transwell filters (Corning Costar) to the chemokines in the bottom chamber as described[57]. Analysis of the formation of B cells synapse on lipid bilayers[28] and *in vitro* B cell–T cell conjugation assays (with peptide-activated OT-II cells and lipopolysaccharide-stimulated B cells)[26] were done as described.

Mapping and sequencing. B6.*cpm* × 129 F_1 mice and B6.*pri* × B10 F_1 mice were intercrossed to generate F_2 progeny, and strain-specific microsatellite and single-nucleotide polymorphism markers were used to map the *cpm* and *pri* loci to chromosome 19. B6.*cpm* × CBA F_2 mice and B6.*pri* × CBA F_2 mice were analyzed to map to a 4.5-megabase interval with the single-nucleotide polymorphism markers rs3697576, rs13483577 and rs3717280. *Dock8* was amplified from genomic DNA or splenocyte cDNA (primer sequences, **Supplementary Table 1**) and was sequenced with ABI Big-Dye terminators and analysis on an ABI 3830 capillary sequencer. Splenocyte cDNA was amplified with primers spanning *Dock8* exons 18–21, then the products were resolved on agarose gels and were subcloned with the TOPO TA Cloning kit (Invitrogen) and the pCR2.1 vector, and individual colonies were amplified by PCR and were sequenced to identify the splicing products produced by the *cpm*/*cpm* mutation.

Data and statistical analysis. GraphPad Prism Software was used for statistical analyses. Unpaired *t*-tests were used for statistical comparison. Data for immunization antibody titers (enzyme-linked immunosorbent assays) were analyzed by nonlinear regression (curve fit) and shift in the half-maximal effective concentration to allow comparison of titration curves.

55. Horikawa, K. *et al.* Enhancement and suppression of signaling by the conserved tail of IgG memory-type B cell antigen receptors. *J. Exp. Med.* **204**, 759–769 (2007).
56. Jun, J.E. *et al.* Identifying the MAGUK protein Carma-1 as a central regulator of humoral immune responses and atopy by genome-wide mouse mutagenesis. *Immunity* **18**, 751–762 (2003).
57. Reif, K. *et al.* Balanced responsiveness to chemoattractants from adjacent zones determines B-cell position. *Nature* **416**, 94–99 (2002).

doi:10.1038/ni.1820